
Spatially Dependent Deadtime Losses in High Count Rate Cardiac PET

Nanette M.T. Freedman, Stephen L. Bacharach, Miles E. McCord and Robert O. Bonow

National Institutes of Health, Bethesda, Maryland and Positron Corporation, Houston, Texas

Cardiac PET scans result in nonhomogeneous distributions of activity within the body, which might lead to great variations in singles rates around the detector ring. Conventional deadtime correction algorithms assume that the singles rates are uniform. This paper investigates singles nonuniformities during several typical cardiac scanning protocols (bolus injections of ^{15}O -water and ^{82}Rb , slow infusion of ^{18}F -FDG and static imaging with FDG) and estimates how such nonuniformities might affect quantitative data. Nonuniformity was observed in all studies and was described by an asymmetry index which increased to 58% during bolus water injection, the most inhomogeneous study. These results are valid for any scanner with a ring diameter of approximately 78 cm and are independent of the amount of activity injected. Deadtime losses depend on the amount of activity and on the scanner type. Nonhomogeneities in singles can be shown to produce spatially dependent deadtime correction factors; for our scanner, these were seen to differ by up to 16% from the mean deadtime correction during bolus water injection. To demonstrate the distortions generated by average deadtime correction, the activity distribution during a clinical cardiac study was simulated using a phantom. A simple local deadtime correction and its implementation on our system are described, and the resulting improvements in both absolute and relative quantitation of the phantom study are shown.

J Nucl Med 1992; 33:2226-2231

In cardiac PET imaging, the distribution of activity in the field of view of the scanner is often nonuniform (1). These nonuniformities cause the count rates around the ring of the scanner to be circularly asymmetric about the center of the field of view. Most deadtime correction schemes, however, assume a symmetrical distribution around the scanner ring. Such deadtime correction schemes may work well when imaging relatively symmetric organs like the brain, but deviations from the assumption of a symmetric activity distribution may lead to errors (2). It is important, therefore, to characterize the degree of asymmetry which may occur during clinical studies. This characterization is especially important in high count rate

dynamic cardiac studies (e.g., ^{82}Rb or ^{15}O -water), where deadtime problems are very severe (3), but may also be important during lower activity dynamic ^{18}F -FDG studies.

This study characterizes the asymmetries of singles count rates around the scanner ring which occur in cardiac ^{15}O , ^{82}Rb and ^{18}F -FDG studies. These observations will be nearly machine-independent for any whole-body PET scanner with a ring diameter of comparable size (~78 cm), although the resulting errors in deadtime correction will be machine-dependent. The asymmetry of singles count rates may change with time during a study; these effects are also examined for dynamic acquisitions (both bolus injection and slow infusion) and for static acquisitions. These data will allow users of various designs of PET scanners to estimate the degree to which their particular scanner may be affected by the asymmetries reported here. An example is presented, using phantom data, which shows how the measured asymmetries can cause errors in deadtime correction. The implications of these errors for the quantitation of clinical cardiac studies are also discussed. Finally, one possible method for correcting the errors resulting from the observed asymmetries is described. While the details of this method are applicable only to the scanner described, the methodology is more generally valid.

METHODS

Patient Data

The principal goal of this study was to examine the distribution of singles rates around the scanner ring during clinical cardiac studies. We studied these distributions in examples of each of three types of study commonly used for quantitative evaluation of cardiac physiology: static acquisition of ^{18}F -FDG, dynamic acquisition of slowly infused ^{18}F -FDG and bolus injection of ^{82}Rb - or ^{15}O -labeled water. The initial phase of the ^{18}F -FDG studies in which the FDG was infused over a period of 60-90 sec was used as an example of a slow infusion. Oxygen-15-water and ^{82}Rb studies provided two examples of bolus injection (bolus injection administered manually over 2-4 sec in the former and over ~20 sec in the latter). The doses injected were 5 mCi for the FDG studies, 15 mCi for the ^{82}Rb , and 20 mCi for the ^{15}O -water. It should be noted that as well as being scanner-independent, as mentioned above, the nonuniformity of singles count rate is also dose-independent, although the resulting deadtime losses are clearly strongly dose-dependent. A map of singles events was collected every second during the initial high count rate part of

Received Nov. 12, 1991; revision accepted Jul. 27, 1992.
For reprints contact: Dr. Nanette Freedman, Dept. Nuclear Medicine, Bldg 10 Rm 1C-401, National Institutes of Health, Bethesda, MD 20892.

the study for the ^{15}O -water studies, every 2 sec for the ^{82}Rb studies and every 5 sec for the ^{18}F -FDG studies. Ten patients were examined for each type of study. The spatial distributions were measured for each patient, and from these data the average distributions of singles rates around the scanner ring were calculated. The resulting deadtime losses for the particular scanner used in this study were also estimated.

Phantom Data

The patient data studies described above provided all the data necessary to characterize the nonuniformities in singles observed around the scanner ring. A phantom study was performed in order to better understand the consequences of these nonuniformities and to investigate a simple deadtime model which might offer some immunity from the effects of nonuniform singles. The phantom consisted of an off-center cardiac insert within an elliptical cylinder (Data Spectrum #2230). The elliptical cylinder also contained two low attenuation cylindrical inserts to represent the lungs. Initially about 30 mCi of ^{18}F were put into the "myocardial" section of the cardiac insert (the section consisting of the 110 ml shell between two domed cylinders). The remainder of the elliptical phantom and of the cardiac phantom insert were filled with nonradioactive water. A series of acquisitions was made without moving the phantom, so that the regional activity in the "myocardium" of the phantom could be estimated at a high count rate and also when, after decay of the ^{18}F , the count rate would be sufficiently low for deadtime correction to be unimportant. The phantom was scanned six times, when the levels of activity within the myocardium were approximately 30, 25, 20, 15, 10 and 5 mCi (activity concentrations of approximately 27.3, 22.7, 18.2, 13.6, 9.1, 4.5 $\mu\text{Ci}/\text{cc}$, respectively). Singles rates were measured every 10 sec throughout all the acquisitions. After allowing the activity to decay to a negligible level, a transmission scan was performed without moving the phantom to permit correction for attenuation.

The studies were reconstructed twice, once with the "standard" mean singles deadtime correction method (which assumed that the singles rates were uniform around the ring) and once with a correction method described below, which did not assume uniform singles around the ring. In both cases, normalization for variation in detector pair efficiency, correction for variation in radial sensitivity, attenuation, randoms, scatter and wobble corrections were applied. Regions of interest were drawn on the images and the activity concentrations in these regions were estimated in order to measure the degree to which regional "myocardial" nonuniformities were introduced by the assumption of a uniform singles rates.

Scanner

This work was carried out on a Posicam PC 6.5 whole-body 21-slice scanner. Characteristics and performance of this scanner have been described in detail elsewhere (4). The Posicam PC 6.5 scanner is made up of a ring of 120 BGO detector modules. Each module is 12 cm in axial extent and 8.5 mm wide and contains 11 crystals as described in reference 4. The diameter of the detector ring is 78 cm and the usable field of view has a diameter of 43.5 cm over an axial length of 11.5 cm. At the conclusion of each acquisition, in addition to a sinogram, a singles file is generated containing the singles data from each detector at user specified time intervals. The temporal resolution of the singles data may be selected to be much finer than the temporal resolution of the sinograms. This feature allowed observation of the

axial and radial variation of the singles over time, even during a static acquisition.

Deadtime Correction

The deadtime correction calculation on the Posicam 6.5 system, like most other scanners, is a mean singles deadtime method, i.e., it assumes a uniform distribution of singles events around the ring. The total singles count rate over all detectors is calculated from the singles data, and the "mean-singles" deadtime correction factor is calculated using an empirically determined function relating average singles rate to deadtime. The empirical function is determined from a series of scans of a decaying 20 cm diameter cylindrical phantom with uniform activity distribution, centered in the field of view. These data are corrected for randoms (detector pair by detector pair) and scatter before the dependence of deadtime correction factor on singles rate is estimated. The entire emission sinogram (corrected for randoms and scatter) is multiplied by this deadtime correction factor.

A preliminary investigation was made of a simple, alternative, spatially dependent deadtime correction scheme, which partially accounts for the variation in singles rates around the ring. This correction scheme, while not perfect, is easily implemented on existing scanners and seems to eliminate a large part of the dependence on singles nonuniformity. Instead of computing one singles deadtime correction factor for the entire emission sinogram, a complete sinogram of deadtime correction factors was created in the following way. The singles rate was measured at each of the eight sectors of the detector ring (each sector comprising a 45° arc). There are 20 possible sector pairs which include all coincidences corresponding to events within the field of view (coincidences between detectors in the same sector or in adjacent sectors are excluded, thus $(8 \times 5/2) = 20$ sector pairs). At each of these 20 pairs of sectors, the mean singles rate and the corresponding "mean-singles" deadtime correction factors for both sectors were computed, and the deadtime correction factor for the sector pair was calculated as the geometric mean of the deadtime correction factors for the sectors making up the pair; this value was recorded in the appropriate locations of a deadtime correction sinogram. Only eight sectors were used, as the singles rates varied only slowly around the ring. The sinogram was blurred by 2.04 cm FWHM Gaussian smoothing to account for wobble, and interpolated to the same 256×120 angle size as the emission sinogram. Each point in the emission sinogram could then be corrected by a multiplicative deadtime factor from the corresponding point in the deadtime correction sinogram. It should be noted that for a uniform singles distribution, the deadtime correction factor sinogram would be uniform, and the spatially-dependent deadtime correction would reduce exactly to the "mean-singles" deadtime correction.

RESULTS

Patient Data

Examples of the spatial distribution of singles around the ring circumference during a ^{15}O -water study on a typical patient are shown in Figure 1. These data were collected 10, 15, 20, 25, 30 and 40 sec following a bolus antecubital injection of ^{15}O -water. There is considerable nonuniformity around the circumferential profile and the spatial distribution of the singles changes with time. Initially, the peak singles are seen to be at the anterior of the

patient, above the right ventricle, which is where most of the activity would be at this time. Then, as the ^{15}O bolus passes from the right ventricle into the left ventricle, the peak singles rate shifts slightly to the left of the patients, and the singles rates become somewhat more widely distributed spatially, although asymmetry remains throughout.

A measure of how nonuniform the singles are around the detector ring at any time can be computed by first calculating the difference between the sector with highest singles (sectormax) and the sector with least singles (sectormin), and then computing the ratio of that difference and the sum (sectormin + sectormax). The index is therefore calculated as:

$$100 \frac{(\text{sectormax} - \text{sectormin})}{(\text{sectormax} + \text{sectormin})} \% \quad \text{Eq. 1}$$

and varies from 0 (for perfect symmetry) to 1 (for maximum asymmetry). This index of spatial asymmetry of singles is plotted against time in Figure 2a, using eight 45° sectors, for the average patient in a ^{15}O -water study shown in Figure 1. The range of values seen among the 10 patients studied is indicated by the bars on the graph. Figure 2a demonstrates that during the initial seconds of the study, immediately after the bolus injection, there is over 60% spatial asymmetry of singles distribution for the average patient. This decreases to about 14% (range 25%–8%) as the activity becomes more widely dispersed with time, and never reaches zero. Note that this asymmetry index does not show which sectors have the greatest or least counts, or if the sectors having the maximum and minimum counts change with time. Figure 2b shows how the asymmetry index varies with time following a ^{82}Rb 30-sec bolus injection. The curve shows the average behavior of a patient, along with the range of values measured over the 10 patient studies. In this case, the initial spatial asymmetry is also high, over 40%, and decreases later in the study to about 10%, (range 14%–6%).

In Figures 2c–d, the asymmetry index is plotted for an ^{18}F -FDG study. Figure 2c shows the changes that occur during the slow infusion phase of the study, while Figure 2d shows the asymmetry during the entire study. The part of the study used to form a static image is from 30 to 60 min postinjection. During this part of the study, the spatial distribution of singles is fairly stable, but not uniform, 12% for the average patient, (range 22%–7%). During the first 20 or 30 sec of the study, the asymmetry reaches a peak nearly as great as that for a bolus ^{15}O -water injection, about 45%.

These asymmetric singles and coincidence rates around the ring will cause data loss which is not homogeneous. Therefore, the usual mean-singles (or even mean-coincidences) based correction schemes will not properly correct for this data loss. This observation is true for all commercially available scanners. For the ^{15}O -water study corresponding to Figure 2a above, the deadtime correction factors that would be generated for the sector pairs with

the minimum and maximum singles rates are plotted for the Posicam 6.5 scanner, together with the mean-singles deadtime correction factors. As described above, the local deadtime correction factor for a sector pair is calculated as the geometric mean of the deadtime correction factors corresponding to the singles count rates at the two sectors making up that pair. Figure 3 clearly shows that the deadtime correction factors based only on mean counts can differ greatly from the deadtime incurred by the sector pairs seeing the bulk of the activity in the heart (the maximum deadtime correction factor curve) and from that incurred by the sector pairs seeing the least amount of activity (the minimum deadtime correction factor curve). At the peak of the curve where the mean deadtime correction factor is about 1.87, the deadtime correction factor for the maximum sector pair reaches 2.19, while the factor for the minimum sector pair is 1.66. These latter values are of course only valid for the Posicam 6.5, but illustrate the general nature of the effect.

Phantom Data

A serious effect of ignoring the spatial dependence of deadtime is the introduction of nonuniformities into the image. The cardiac phantom study was used to evaluate the severity of such nonuniformities in cardiac imaging. The mean singles asymmetry index for the phantom study was 30%, which is within the range of values seen for the human studies in Figure 2 for water, rubidium and FDG. The variation of deadtime correction factors by sector pair as the activity decayed is shown graphically (Fig. 4). While the mean deadtime correction factor only reaches a value of 2.4, the largest local deadtime correction factor reaches 5.2. To illustrate the extent to which ignoring the spatial dependence of deadtime can result in errors in absolute and regional quantitation, the series of images of the myocardial phantom at activities 30, 25 and 5 mCi are shown in Figure 5a. In Figure 5b, the same series of images is shown, but this time processed with local deadtime correction. The images at the higher activities show much lower absolute counts, when processed with spatially averaged deadtime correction, as demonstrated in Figure 5a. In Figure 5b, it can be seen that with local deadtime correction, this effect is less severe. To illustrate the regional effects, two regions were drawn in the myocardium, indicated as A and B in Figure 5a. At a low activity (5 mCi), the ratio of counts in regions A and B was the same (nearly unity), regardless of the deadtime correction scheme used—mean or local. At high activity this ratio changes by only 2% for local deadtime correction, but by 15% when mean deadtime correction was used. Therefore, the local deadtime correction results in very little change at high activity, whereas the mean deadtime correction introduces spatial inhomogeneities. Again these deadtime values are applicable only to the Posicam 6.5, but the trend is generally applicable.

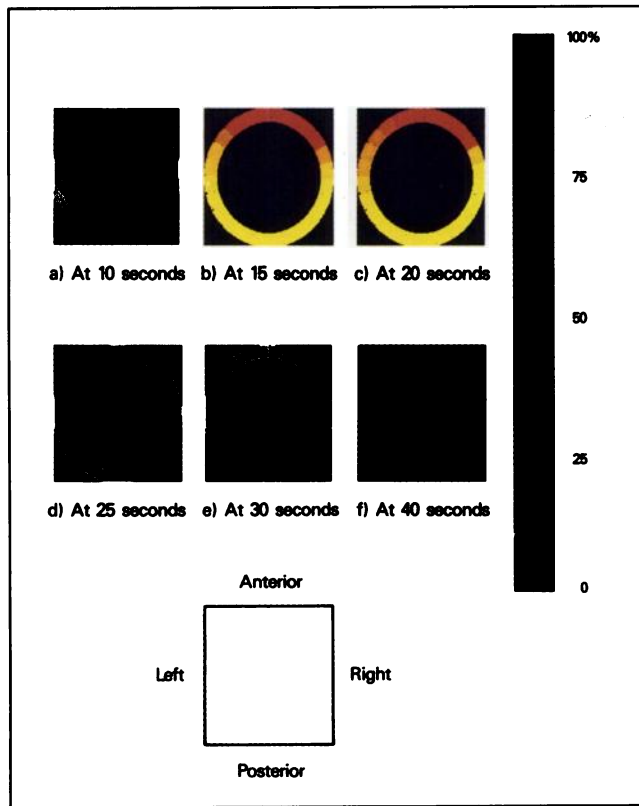


FIGURE 1. Changes in spatial distribution of singles during a dynamic ^{15}O -water study, shown as % maximum singles rate.

DISCUSSION

Bolus injections of activity and even slow infusions result in very large spatial asymmetries of singles count rates around the ring. This is demonstrated dramatically in Figure 2 for actual clinical cardiac studies. As expected, the asymmetry in singles rate is most severe in the initial

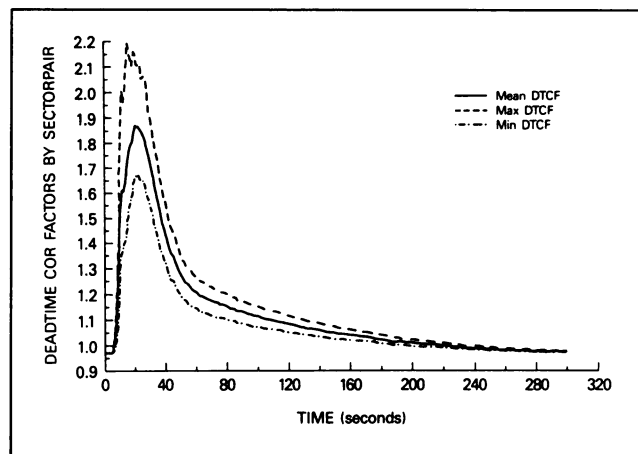


FIGURE 3. Minimum, maximum and mean deadtime correction factors for permitted sector pairs for ^{15}O -water bolus injection study.

phase of a bolus injection, as the activity passes in a gradually spreading bolus through the chambers of the heart and into the myocardium. The large asymmetry during the early phase of the study can be expected to cause errors in arterial activity concentration curves. These errors will be time-dependent, as the degree of spatial variation itself changes with time.

It is also apparent that some asymmetry is present even during static FDG imaging. While this static asymmetry may not prove to be important for the relatively small amount of activity injected for FDG imaging, it may be very important for static images of higher activity, as with ^{13}N -ammonia (5).

Asymmetry in singles and coincidence rates will depend on the distribution of activity and the attenuation. The activity distribution will partly be determined by the char-

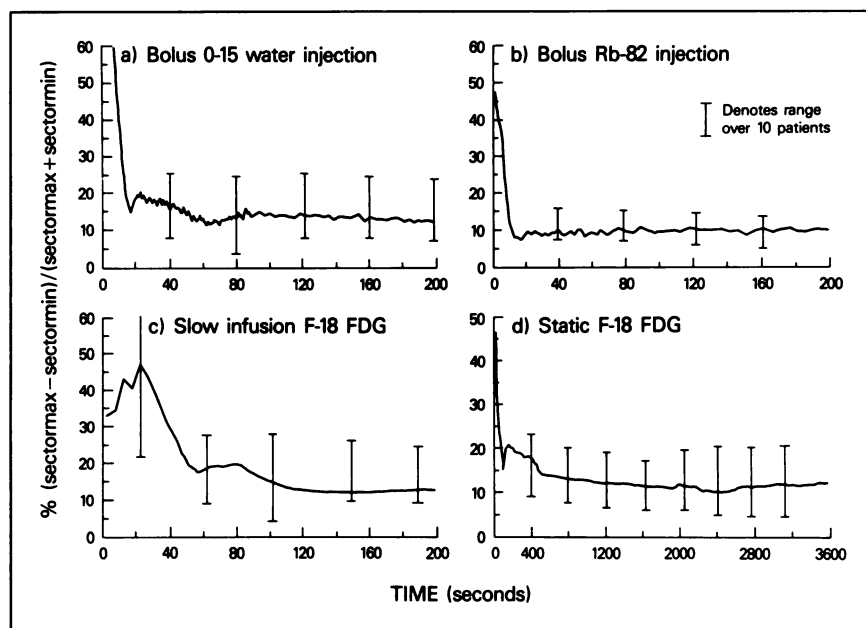


FIGURE 2. Asymmetry index for spatial distribution of singles around scanner ring. (a) Bolus injection of ^{15}O -water, (b) bolus injection of ^{82}Rb , (c) slow infusion of ^{18}F -FDG and (d) static ^{18}F -FDG.

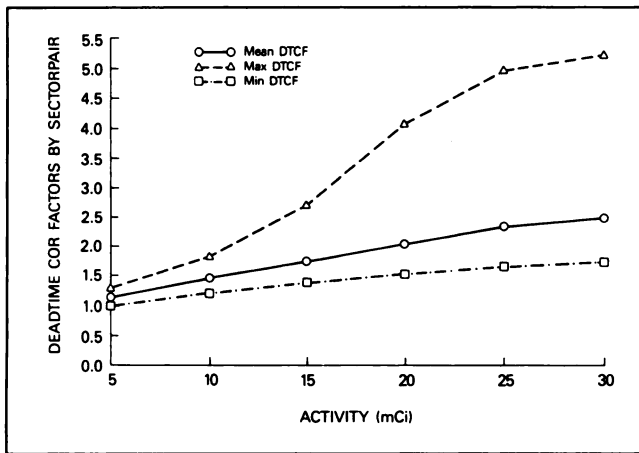


FIGURE 4. Minimum, maximum and mean deadtime correction factors for permitted sector pairs during ^{18}F myocardial phantom study.

acteristics of the labeled compound, but will also vary to some extent from patient to patient, as seen from Figure 2 where the range over 10 patients as well as the values for an average patient are shown. The physiology (e.g., transit time differences) and anatomy of the patient will affect the spatial and temporal distribution of activity. In addition, the size and shape of the patient will determine the

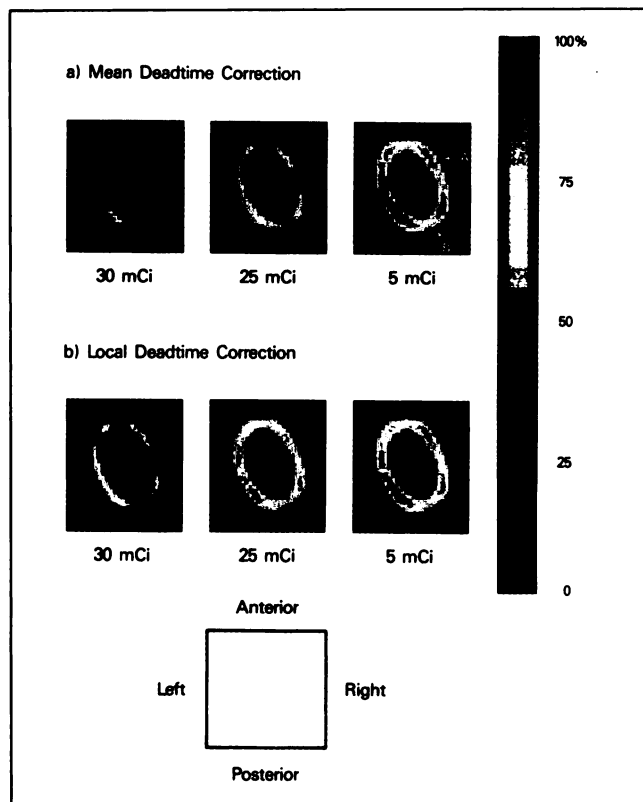


FIGURE 5. Images of myocardial phantom processed with (a) mean and (b) local deadtime correction scaled to % maximum counts per pixel.

magnitude and distribution of attenuation. These variations between patients are likely to be much greater for cardiac scans (or other whole-body scans) than for brain scans.

The effects of asymmetric count rate on deadtime losses will be machine dependent. They will depend on exactly how the processing of detected counts is performed, how much of the processing circuitry is shared between signals coming in at different locations around a detector ring or throughout the field of view, and on what the rate-limiting steps in the processing are. Regardless of where these rate-limiting steps are, an asymmetric activity distribution may yield local count rates high enough to result in significant local deadtime losses even when the deadtime calculated from average count rates is low. The individual differences between patients indicate that corrections for locally varying deadtime losses should be based on the actual spatial distribution of count rates (in our case obtained from singles) rather than on a local deadtime model derived from a phantom.

For the particular scanner used here, deadtime correction factors as large as 1.85 were computed from clinical studies, based on average singles rates. However, the deadtime correction factors corresponding to the minimum and maximum count rate sector pairs have local deadtime correction factors of 1.65 and 2.2, respectively. Use of the average deadtime correction factor in the usual way to multiply all parts of the sinogram would therefore cause the counts registered in the minimum sector pairs to be overestimated, and the counts registered in the maximum sector pairs to be underestimated, by up to 16%. This could of course lead to image distortion, the magnitude of which would be more severe with injection of more activity.

The phantom study was designed to have asymmetry comparable to that seen in clinical studies, and to demonstrate the absolute errors and regional inhomogeneities which could be produced if deadtime correction is performed while ignoring the effects of such spatially varying singles rates. In the phantom study, the variations in singles count rates were comparable to those seen in clinical studies. The sector pair count rate variation index was approximately 30%–40%. Similar levels were seen in the clinical studies, during bolus injection and slow infusion of activity. Since the initial activity in the phantom (30 mCi) was deliberately chosen to be higher than the highest doses currently used for cardiac PET scans at our institution [though comparable to doses used by some other investigators (6,7)], deadtime losses are initially much greater than those seen in our clinical studies. Initially with 30 mCi all in a small myocardial phantom, there is an average deadtime correction factor of 2.4, but deadtime factors for the permitted sector pairs with least and greatest count rates are 1.8 and 5.2, respectively. However, at 15 mCi, the mean, minimum and maximum deadtime correction factors (1.7, 1.2 and 2.6, respectively) are compa-

able to those seen during clinical studies, though the range is somewhat larger, possibly because in the clinical situation, even in the initial phase after a bolus injection, the activity is never concentrated so exclusively into a small area.

Estimates of decay-corrected activity concentration when the phantom study is processed with the regular average deadtime correction are seen to be very severely underestimated at high activities (Fig. 5), and inhomogeneities are also introduced. These errors are much improved by local deadtime correction. Application of the simple local deadtime correction method resulted in estimates closer to the low activity values for all activities, and inhomogeneities were less marked.

The spatial variation of count rates and of deadtime losses were comparable in the phantom study and in the clinical studies. This suggests that in the clinical studies, as in the phantom, there may be substantial errors in both absolute and relative estimates of activity concentration in regions of interest in the image due to use of average deadtime correction. These phenomena will be most severe when high activities are injected and during the initial phases of either a bolus injection or slow infusion.

CONCLUSION

It has been shown that the most commonly employed cardiac imaging procedures produce a singles and coincidence count rate which is highly nonuniform about the detector ring. This is true regardless of whether the injection is a rapid bolus or a slow infusion. The most severe asymmetry occurs during the initial phase of a bolus injection study, but some asymmetry persists throughout the study and occurs even for static images. Most deadtime correction schemes, however, assume uniform singles and

coincidence rates around the detector ring. This implies that whenever local count rates are sufficient to cause deadtime losses, one must use deadtime correction schemes that recognize these local variations. Use of deadtime correction schemes based on mean singles rates ignores these local variations. This study has shown that this could lead not only to errors in the estimates of absolute activity but also to regional errors in the final image. The phantom study described here confirms that errors in relative as well as in absolute values can occur. Application of a simple, local deadtime correction method reduced the errors in both relative and absolute quantitation for the particular scanner under study. This method or a variant may well be applicable to other scanners as well.

REFERENCES

1. Bacharach S, Freedman N, McCord M, Bonow RO, Dilsizian V, Cuocolo A. The effect of spatially dependent deadtime on cardiac PET imaging. *J Nucl Med* 1990;31:777-778.
2. Daube-Witherspoon ME, Carson RE. Unified deadtime correction model for PET. *IEEE Trans Med Imag* 1991;10:267-275.
3. Thompson CJ, Meyer E. The effect of live time in components of a positron tomograph on image quantification. *IEEE Trans Nucl Sci* 1987;34:337-343.
4. Mullani NA, Gould KL, Hartz RK, et al. Design and performance of Posicam 6.5 BGO positron camera. *J Nucl Med* 1990;31:610-616.
5. Hutchins GD, Schwaiger M, Rosenspire KC, Krivokapich J, Schelbert H, Kuhl DE. Noninvasive quantification of regional blood flow in the human heart using N-13 ammonia and dynamic positron emission tomographic imaging. *J Am Coll Cardiol* 1990;15:1032-1042.
6. Bergmann SR, Herrero P, Markham J, Weinheimer CJ, Walsh MN. Noninvasive quantitation of myocardial blood flow in human subjects with oxygen-15-labeled water and positron emission tomography. *J Am Coll Cardiol* 1989;14:639-652.
7. Herrero P, Markham J, Shelton ME, Weinheimer CJ, Bergmann SR. Noninvasive quantification of regional myocardial perfusion with rubidium-82 and positron emission tomography. *Circulation* 1990;82:1377-1386.